Organic & Biomolecular Chemistry

Cite this: *Org. Biomol. Chem.*, 2012, **10**, 6973

www.rsc.org/obc

PAPER

Fluoride-responsive gelator and colorimetric sensor based on simple and easy-to-prepare cyano-substituted amide†

Yuping Zhang and Shimei Jiang*

Received 24th May 2012, Accepted 10th July 2012
DOI: 10.1039/c2ob26016f

A new and easy-to-prepare gelator based on cyano-substituted amide (BPNIA) was designed and synthesized. BPNIA could form thermoreversible gel in DMSO–H_2O (v/v, 9 : 1) and ultrasound-stimulated gel in DMSO. FT-IR, UV–vis and XRD spectra indicated that the gelator molecules self-assemble into a fibrous network resulting from the cooperation of intermolecular hydrogen bonding, π–π stacking and cyano interactions. BPNIA can act as a highly selective colorimetric sensor for fluoride in DMSO, overcoming the interference of $H_2PO_4^-$, AcO^- and other halide anions. The deprotonation of the NH groups is responsible for the dramatic color change from colorless to yellow. Interestingly, the organogel of BPNIA could allow a two channel fluoride response by proton controlled reversible sol–gel transition and color changes.

Introduction

There has been an increasing amount of interest in low-molecular-mass organic gelators (LMOGs),[1] which is motivated by their unique supramolecular architectures and wide range of potential applications. Organogels are formed by assembly of LMOGs into entangled three-dimensional networks through weak intermolecular forces such as hydrogen bonding, π–π stacking, and van der Waals interactions in which solvent molecules are efficiently entrapped and immobilized.[2] These weak intermolecular forces can be easily manipulated by external stimuli, allowing for the tuning of the physical properties of the gel. To date, a great number of examples based on organogels that respond to pH,[3] anions,[4] redox agents,[2c,5] electric or magnetic fields,[6] light[7] and sound,[8] have been reported. Such stimuli-responsive gels are especially beneficial for the development of sensor devices or in applications like drug delivery or catalysis. Hence, the design of simple and easy-to-prepare stimuli-responsive gelators is worth exploring.

Anions are ubiquitous and play a crucial role in a wide range of chemical and biological processes. Among various anions, fluoride is a useful chemical for dental caries and treatment of osteoporosis, but too much accumulation of fluoride can result in fluorosis.[9] Therefore, a great deal of attention has been devoted to the detection of fluoride.[10] Optical colour changes as a signaling event, employing synthetic receptors, are widely used owing to their simplicity, low cost and no equipment requirements. However, most of them suffer the interference of other anions. Specifically, the discrimination of fluoride from $H_2PO_4^-$ and AcO^- with similar basicity is rather problematic.[11] So, it is still a challenge to design and synthesize artificial sensors with high selectivity and sensitivity for fluoride anions. Furthermore, these fluoride sensors commonly are used in solution, which will significantly restrict their practical applications. Faced with these limitations, anion-responsive gels have attracted increasing attention because the gel–sol transition allows naked eye detection and the gels are more convenient to use. Till now, the reports of organogels displaying fluoride response are still limited.[2b,12] Therefore, it is desirable to develop fluoride-responsive organogels that could display two channel recognition of fluoride through gel–sol transition and color changes with the advantage that these responses can be conveniently detected by the naked eye.

In this work, we designed and synthesized a new fluoride-responsive gelator based on cyano-substituted amide which lacks steroidal units and long alkyl chains, as shown in Scheme 1. The synthetic strategy stems from the fact that a cyano-substituted aromatic amide with strong intermolecular hydrogen bonding and π–π stacking may provide powerful driving forces to form an organogel.[2b,13] On the other hand, the two NH groups of the amide can act as anion acceptors and the cyano-substituted aromatic groups can be utilized as the chromophore that converts the interaction between hydrogen atom and anion to optical signals.[14] Finally, the cyano electron-withdrawing groups can further polarize the NH group and enhance the hydrogen bond donor tendencies toward anions. Indeed, our compound not only acts as a smart gel that shows reversible gel–sol transition and a

State Key Laboratory of Supramolecular Structure and Materials, Jilin University, 2699 Qianjin Avenue, Changchun 130012, P.R. China. E-mail: smjiang@jlu.edu.cn; Fax: +86-431-85193421; Tel: +86-431-85168474

†CCDC 883025. For crystallographic data in CIF or other electronic format see DOI: 10.1039/c2ob26016f

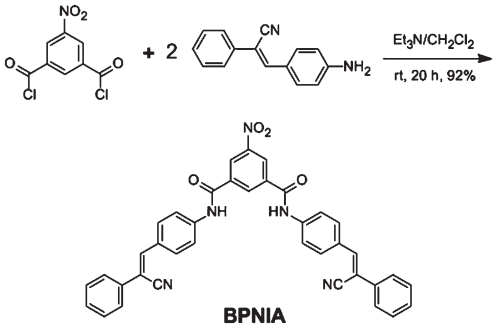

Scheme 1 Synthesis route to gelator BPNIA.

visibly noticeable color change controlled by using fluoride stimuli and proton control, but also exhibits a highly selective sensing activity *versus* fluoride in DMSO solution and overcomes the interference of $H_2PO_4^-$, AcO^- and other halide anions. To the best of our knowledge, only a few reports on LMOGs showing a significant dual channel fluoride ion response of reversible color change and gel–sol transition are known.[12a,d,f] Therefore, the cyano-substituted amide is a good example of a fluoride-responsive gelator, which may be important to provide structural criteria for the deliberate design of new, easy-to-prepare stimuli-responsive gelators with potential applications in sensor devices for fluoride detection.

Results and discussion

Synthesis and crystal structure of BPNIA

The structure and synthesis of the cyano-substituted amide BPNIA is shown in Scheme 1. It was easily synthesized in good yield by condensation of 5-nitro-isophthaloyl dichloride with 2-phenyl-3-(*p*-aminophenyl)acrylonitrile in the presence of triethylamine, and characterized by ^{1}H NMR, MS, FT-IR and elemental analysis.

A single crystal of BPNIA suitable for X-ray crystallography was obtained with slow evaporation of its DMF solution at room temperature. The crystal structure is triclinic with space group $P\bar{1}$, two independent BPNIA molecules exist in a unit cell and each of them is in contact with two DMF molecules through intermolecular hydrogen bonding. All the NH groups of BPNIA, as donors of hydrogen bonds, interact with the oxygen atom of DMF. According to meticulous inspection of the BPNIA packing arrangement, strong intermolecular interactions exist among BPNIA molecules. As shown in Fig. 1b, the molecules self-assemble into one-dimensional (1D) chains along the *a* axis, where hydrogen bonds of C–H···N≡C, C–H···O=C and π–π stacking are responsible for the formation of such molecular assemblies with a less optimal way of J-aggregate molecular stacking mode. The interaction distances of hydrogen bonds H···N, H···O and π–π are 2.663, 2.430 and 3.418 Å, respectively, meaning that these intermolecular interactions are relatively strong. Furthermore, two types of C–H···O=C and C–H···N≡C hydrogen bond are bound along the *b* axis in the crystal molecules, these distances are 2.646 and 2.748 Å, respectively (Fig. 1c). Driven by these strong intermolecular interactions, the molecules of BPNIA self-assemble into tight two-dimensional layer frameworks.

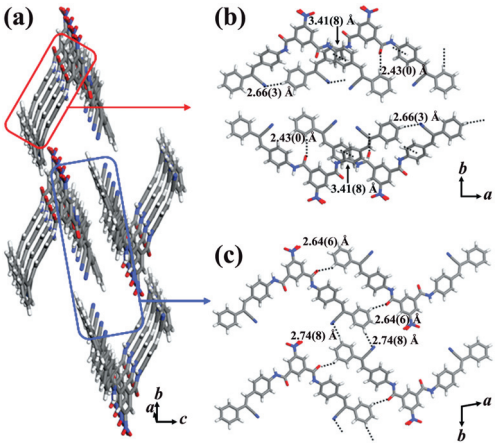

Fig. 1 (a) Molecular packing of BPNIA along the *a* axis; DMF molecules are omitted for clarity. (b) C–H···N≡C, C–H···O=C and π–π interactions viewed along the *ab* plane. (c) C–H···N≡C and C–H···O=C interactions between adjacent molecules.

Table 1 Gelation properties of BPNIA in various solvents[a]

Solvent	Phase	Solvent	Phase
n-Hexane	I	Ethyl acetate	I
Cyclohexane	I	Toluene	I
Dichloromethane	I	THF	I
Chloroform	I	DMF	S
Methanol	I	DMSO	S
Ethanol	I	DMSO–H_2O (9 : 1)	G (12)
Acetonitrile	I	DMSO	G (24)[b]

[a] S, solution; G, stable gel; I, insoluble. Numbers in parentheses present the critical gel concentration (CGC, mg mL^{-1}). [b] Gel induced by ultrasonic stimulation.

Gelation property of BPNIA

The gelation abilities of BPNIA were evaluated in various organic solvents by the standard heating-and-cooling method and summarized in Table 1. The compound BPNIA was insoluble in aliphatic hydrocarbon solvents, lower alcohols and aromatic solvents, such as *n*-hexane, cyclohexane, chloroform, methanol and toluene at room temperature, but was easily dissolved in DMF and DMSO. The gelation properties of BPNIA in DMSO were further investigated. Cooling of a thermally dissolved DMSO solution of BPNIA resulted in precipitation; however, when ultrasound irradiation was introduced into the system, it could form stable gels in pure DMSO. These implied that ultrasound may cause desolvation of BPNIA and trigger the gelation.[12h,15] Furthermore, BPNIA can form thermoreversible gels in DMSO–H_2O (v/v, 9 : 1). The gel–sol transition temperatures (T_{gel}), determined by the 'inverse flow method',[16] were 62 °C in DMSO–H_2O (12 mg mL^{-1}) and 46 °C in DMSO (30 mg mL^{-1}). The formed BPNIA gels were quite stable and

could be preserved for more than half a year at room temperature without phase separation.

The morphologies of BPNIA xerogels were obtained by freeze-drying them and examining with a scanning electron microscope (SEM). The microscopic observations revealed that the BPNIA molecules exhibited an outstanding 1D self-assembling tendency. The xerogel from DMSO–H_2O consisted of numerous intertwined fibers with diameters of 50 nm, entangled to form networks sustaining solvent therein (Fig. 2a). In the DMSO xerogel, a large amount of long, flat and thick fibers could be observed, with a high aspect ratio, width of 180 nm and length of tens of micrometres (Fig. 2b). The slight differences among the general characteristics of these 1D architectures might arise from the fact that the fabrication methods and conditions are different for these two xerogels. The formation of elongated fiber-like aggregates indicated that strong directional intermolecular interactions are responsible for the self-assembly of BPNIA molecules.

In order to confirm that the intermolecular interactions play a significant role in the gelating process, UV–vis, FT-IR and XRD spectra of BPNIA xerogels were obtained. The UV–vis absorption spectra of BPNIA in DMSO solution and xerogels states were determined to gain information on the organization of the chromophores. As shown in Fig. 3, the dilute solution of BPNIA with 10 μM in DMSO gave a strong absorption maximum at 355 nm, whereas this peak broadened and a new broad shoulder at 420 nm was detected in the xerogels. It is well known that J-aggregates where the molecules are arranged in a head-to-tail direction induce a red-shift in absorption. The new shoulder band is properly assigned to the J-aggregation band due to specific arrangements by the cyano group.[13,17] These results indicated that π–π stacking plays a key role in gel formation and that BPNIA might adopt J-aggregates in the gel states. This is consistent with the arrangement of BPNIA molecules in the crystals.

FT-IR spectra were measured to focus on the role of the cyano and amide units in the formation of the observed fibers. Fig. 4 compares the IR spectra of the powder and the xerogels of BPNIA. In the powder, the cyano stretching band appears at 2217 cm^{-1}. But the corresponding bands shifted to 2210 cm^{-1} in the case of xerogels, which is due to the results of intermolecular cyano interactions in the gel states, as previously reported.[18] In addition, the NH and CO stretching vibrations in the powder appeared at 3340, 1684 and 1673 cm^{-1}, respectively, while these peaks became broad and shifted to lower wavenumbers at 3307, 1681 and 1669 cm^{-1} in the BPNIA xerogels, suggesting that intermolecular hydrogen bonds exist in the gel states.[2d,12c] In order to further investigate the intermolecular hydrogen bonds between amide groups, we carried out the temperature-dependent FT-IR spectra. As shown in Fig. 5, with the temperature increasing, the band at 3307 cm^{-1} gradually declined and a new band at 3335 cm^{-1} appeared and increased synchronously. This was attributed to the destruction of intermolecular hydrogen bonds, causing the NH position to move to

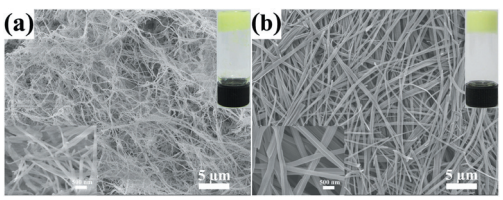

Fig. 2 SEM images of BPNIA xerogels formed from (a) thermal-induced gelation in DMSO–H_2O (v/v, 9 : 1) and (b) ultrasound-stimulated gelation in DMSO. Insets in (a) and (b) show the corresponding magnified SEM image and the organogel.

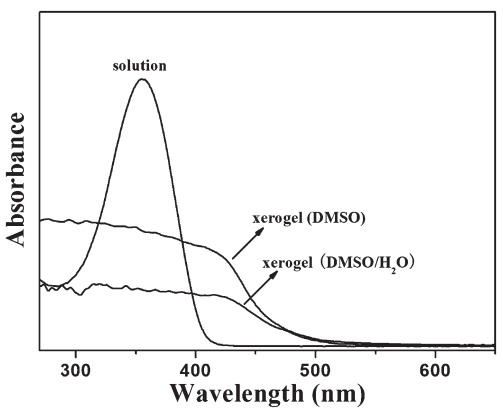

Fig. 3 UV–vis absorption spectra of BPNIA in DMSO solution (10 μM) and xerogels.

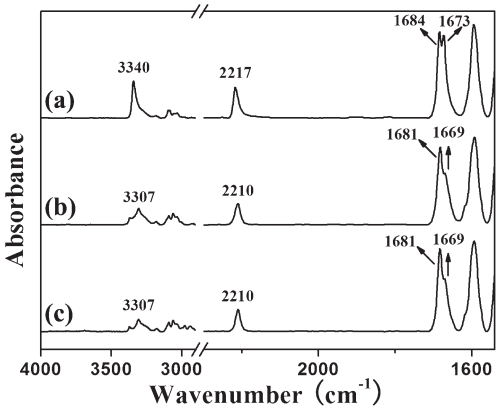

Fig. 4 FT-IR spectra of BPNIA (a) powder; (b) xerogel from DMSO and (c) xerogel from DMSO–H_2O (v/v, 9 : 1) at room temperature.

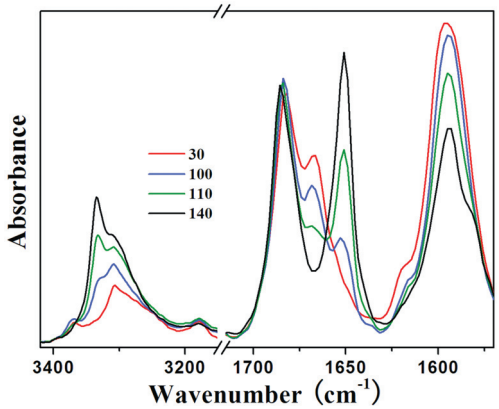

Fig. 5 Temperature-dependent FT-IR spectra of xerogel from DMSO (15 mg/0.5 mL).

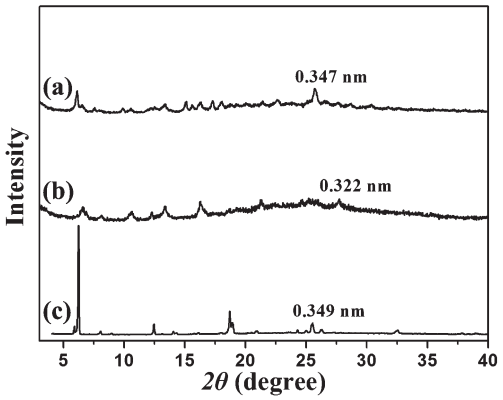

Fig. 6 XRD patterns of BPNIA (a) xerogel obtained from DMSO; (b) xerogel obtained from DMSO–H_2O (v/v, 9 : 1) and (c) crystal.

a higher wavenumber. Moreover, the band at 1681 cm^{-1} shifted to a higher wavenumber, the band at 1669 cm^{-1} gradually decreased, and a new band at 1651 cm^{-1} appeared. These observations clearly show that most of the amide groups were involved in intermolecular hydrogen bonds and promoted the aggregation of BPNIA molecules to form gel. We assume that the intermolecular hydrogen bonds and cyano interactions may both contribute to the gel formation.

XRD was used to explore the regularity of molecular packing and the gelation mechanism of BPNIA in the gel phase. Fig. 6 shows the XRD patterns of BPNIA in xerogels and crystal state. Compared with the crystal of BPNIA, a series of sharp peaks were observed in the BPNIA xerogels formed in DMSO and DMSO–H_2O, demonstrating a typical feature of crystalline-like order structure, which suggested the ordered arrangements of BPNIA in the gel states. In addition, the crystal exhibited an obvious peak at $2\theta = 25.5°$ corresponding to a d spacing of 0.349 nm, a typical π–π stacking distance,[12a,c] which was consistent with the distance between phenyl rings in the crystal phase. Similarly, prominent reflection peaks corresponding to d spacing of 0.347 and 0.322 nm were observed from xerogels of DMSO and DMSO–H_2O, respectively. These results supported that π–π stacking interaction was involved in their self-assembled structure. On the basis of UV–vis, FT-IR and XRD data, it was reasonable to suggest that the driving forces for gelation followed by entanglement of the self-assembled nanofibers resulted from the combined effects of intermolecular hydrogen bonds, π–π stacking and cyano interactions.

Anion responsive properties

It is well known that the amide is an especially good hydrogen bond donor and excellent anion receptor.[10c,19] In order to investigate the interactions of receptor BPNIA with anions, the characteristic UV–vis absorption changes have been obtained after addition of TBA salts of F^-, Cl^-, Br^-, I^-, $H_2PO_4^-$ and AcO^- to its DMSO solution. As can be observed in Fig. 7a, in the presence of 100 equiv of F^-, the absorption band at 355 nm vanished, and a new absorption band appeared at 459 nm. However, $H_2PO_4^-$, AcO^- and other halide anions did not induce any significant spectral changes, suggesting no bonding or very weak

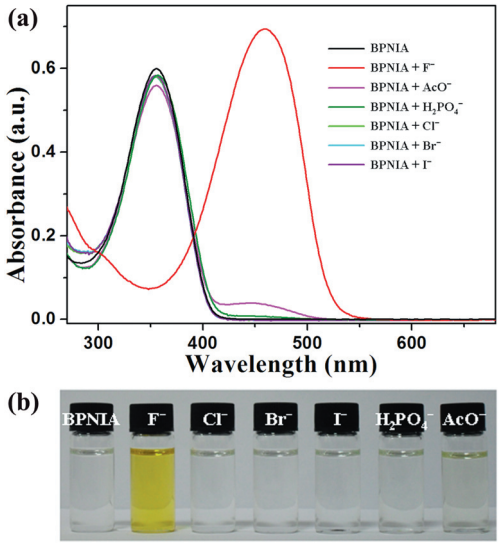

Fig. 7 (a) Absorbance spectra and (b) the corresponding color changes of BPNIA (10 μM) upon addition of 100 equiv various anions in DMSO.

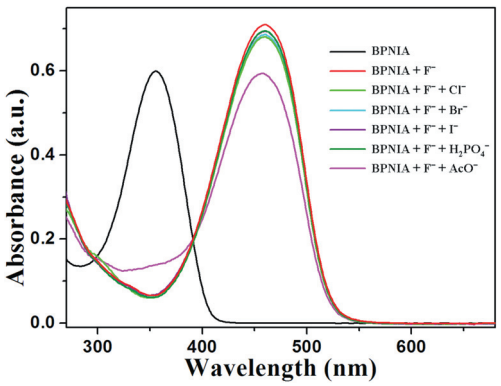

Fig. 8 Absorption spectra changes of BPNIA (10 μM) to F^- (100 equiv) in the absence and presence of 100 equiv of various anions in DMSO.

interactions with the receptor BPNIA. Due to the appearance of a new band in the visible region, the addition of fluoride can cause a vivid color change. As expected, the addition of fluoride led to a noticeable color change from colorless to yellow, whereas no color changes were observed when the other anions were added (Fig. 7b). This suggests that BPNIA allowed highly selective fluoride detection visually.

More importantly, further studies suggested that BPNIA could selectively detect fluoride even in the presence of other competitive anions, and the monitor effect was almost not affected (Fig. 8). The selectivity of fluoride over other anions, in particular $H_2PO_4^-$ and AcO^-, is important because many reported fluoride colorimetric sensors suffered from deleterious interference of other anions.[11]

The interaction of BPNIA with fluoride was investigated in detail through absorbance spectra titration experiments and intricate spectral behaviors were observed (Fig. 9). On addition of from 0 to 25 equiv fluoride, the band at 355 nm decreased, while

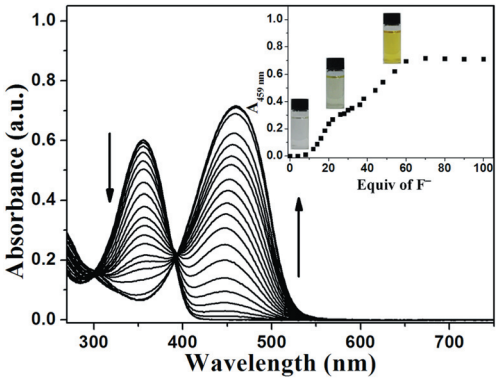

Fig. 9 Absorbance spectra changes of BPNIA (10 μM) upon the addition of 0–100 equiv fluoride in DMSO. Insert: the absorbance changes at 459 nm as a function of fluoride and images of BPNIA with different amounts of fluoride (left: none; middle: 25 equiv fluoride; right: 60 equiv fluoride).

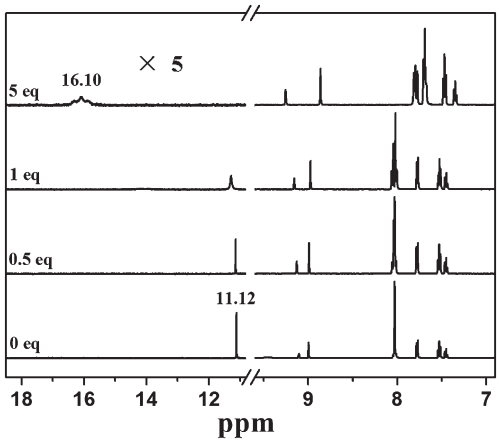

Fig. 10 Plots of ^{1}H NMR spectra of BPNIA upon the addition of fluoride in DMSO-d_6. The ×5 is the scale factor used for the region of 10.5–18.5 ppm.

a new band at 447 nm formed and developed. In particular, the band at 447 nm almost reached the maximum value after the addition of 25 equiv of fluoride. In the meantime, a faint yellow color was observed (Fig. 9, inset). The changes suggested that fluoride first formed a hydrogen bonding complex with BPNIA. With further increasing of the concentration of fluoride from 25 to 60 equiv, the band intensities at 447 nm progressively increased, and a clear red shift of the maximum from 447 to 459 nm could be observed. The band at 459 nm reached its limiting value after the addition of 60 equiv of fluoride, and simultaneously the solution became bright yellow color (Fig. 9, inset). These subsequent changes might result from deprotonation of the amide NH group by the basic fluoride ion, and development of a negatively charged amide.[11g] The deprotonation will be further confirmed through the ^{1}H NMR titration experiments in DMSO-d_6. These results revealed that the deprotonation was the key factor triggering the chromogenic effect. Such deprotonation was related to the strong acidity of the receptor caused by the cyano electron-withdrawing groups and the particular stability of the $[HF_2]^-$.[20]

The interaction of receptor BPNIA with fluoride was further investigated by ^{1}H NMR titration experiments in DMSO-d_6 (Fig. 10). The amide NH proton signal at 11.12 ppm shifted downfield slightly and broadened with increasing fluoride concentration from 0 to 1 equiv. When 5 equiv of fluoride was added, the NH proton signal finally disappeared and a new signal emerged at 16.10 ppm with a 1 : 2 : 1 triplet peak, which was ascribed to the $[HF_2]^-$ dimer.[21] The existence of this new species confirmed the deprotonation of the amide NH group. Consequently, the deprotonation of the NH group brought electron density onto the cyano-substituted aromatic framework, and the protons of the cyano-substituted aromatic moiety distinctly shifted upfield.[22]

Fluoride-responsive gels

From the above discussions, it is interesting to note that the intermolecular hydrogen bonding of amide units is one of the main driving forces that supports gel formation. At the same time, amide units also act as binding sites in anion recognition. Therefore in BPNIA gel, if the hydrogen bonding donor NH sites in the amide units interacted with fluoride, the gelators might not form stable assemblies, resulting in the transformation of the gels, into a solution. The photographs of the gel-to-sol conversion of BPNIA in the presence of fluoride are shown in Fig. 11. After 2 equiv of solid TBAF was carefully added onto the top of the DMSO gel, a thin layer of red solution immediately appeared at the upper part. As time passed, the pale yellow gel gradually vanished and more and more red-colored solution appeared until all the gel transferred into solution. The presence of fluoride not only changed the color of the system but also disrupted the preformed gel to a solution through slow diffusion of fluoride. The results indicated that BPNIA gel is very sensitive to fluoride, with naked eye sensing by gel–sol transition and obvious color changes. Because of the commonality of amide units between organogelator and anion receptor, it was reasonable to attribute the fluoride triggered gel–sol transition to the disruption of hydrogen bonding interaction between the amide groups that results in the dissociation of BPNIA gel network structures and the release of entrapped DMSO. The striking color changes originated from the cyano-substituted aromatic groups as the chromophore converts the deprotonation of the amide moiety with fluoride to optical signals.[11g,14]

The binding between fluoride and the amide units of BPNIA led to gel–sol transition and color changes. On the other hand, it is well known that there is a strong interaction between fluoride and the protic solvent, which could weaken the binding between

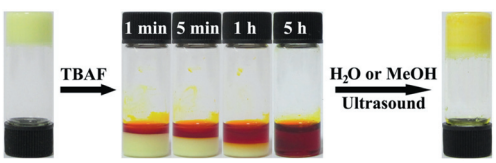

Fig. 11 The changes in the DMSO gel (15 mg/0.5 mL) after addition of solid TBAF (2 equiv). The disintegrated solution could re-gelate after addition of H_2O or methanol under ultrasound.

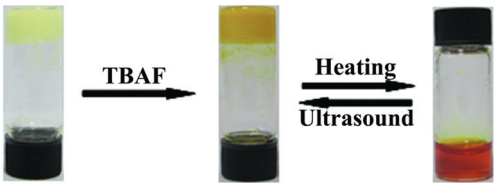

Fig. 12 Photographs of BPNIA gel formed in DMSO–H_2O (v/v, 9 : 1) (9 mg/0.5 mL) and the gel retained by adding 2 equiv of TBAF.

fluoride and amide units. As anticipated, when 0.07 mL of H_2O was added to the red solution formed by fluoride disintegrated gel, a new gel was obtained again after brief sonication and the red color faded (Fig. 11). The addition of 0.15 mL methanol produced similar changes. The recovered BPNIA gel may be ascribed to the fact that protic solvent competes with the amide NH group for fluoride and prevents the deprotonation of amide groups by the fluoride. So the addition of polar protic solvents could make the solution re-gelate and the red color fade.

As mentioned above, the BPNIA gelator could also form stable gels in water-containing medium (DMSO–H_2O, v/v, 9 : 1). The fluoride-responsive properties of BPNIA gel formed in water-containing medium were then studied. After 2 equiv of solid TBAF was carefully added onto the top of the DMSO–H_2O gel, the gel state could be preserved (Fig. 12). To exclude the diffusion factor, we heated the mixture of DMSO–H_2O gel and 2 equiv of fluoride until it became a homogeneous solution, which makes fluoride fully interact with BPNIA. A stable gel was gained as the solution cooled to room temperature under ultrasound treatment. The presence of protic solvent disfavors the interaction between fluoride and amide units of BPNIA.

Hence, BPNIA can act as a smart gel that reversibly gel–sol transitions as well as noticeably changes color by the use of fluoride stimuli and proton control. This is of immediate relevance as the gel-based systems could act as a convenient and efficient fluoride sensor with dual-channel response of gel–sol transition and color changes.

Conclusions

A new gelator BPNIA based on cyano-substituted amide without steroidal units and long alkyl chains was synthesized. It is a rare receptor that allows for the colorimetric detection of fluoride in DMSO and overcomes the interference of $H_2PO_4^-$, AcO^- and other halide anions. BPNIA could form thermoreversible gel in DMSO–H_2O and ultrasound-stimulated gel in DMSO, which was attributed to the cooperative interplay of intermolecular hydrogen bonding, π–π stacking and cyano interactions as shown by FT-IR, UV–vis and XRD studies. Introducing of fluoride not only changed the color of the system but also disrupted the preformed gel to a solution. Subsequently, the addition of polar protic solvents could make the solution re-gelate and the red color fade. So the reversible gel–sol transition and noticeable color change were controlled by the use of fluoride stimuli and proton control. It provides a strategy to design a novel gelator for constructing stimuli responsive soft materials and could lead to potential applications in sensor devices for anion detection and the drug industry.

Experimental section

Materials

Benzyl cyanide (98%), 4-nitrobenzaldehyde (98%) and 5-nitro-isophthalic acid (98%) were obtained from Aldrich. All of the reagents and solvents were analytical reagent grade and used as received without further purification.

Instrumentation

^{1}H NMR spectra were obtained using a Bruker AVANCE 500 MHz spectrometer (tetramethylsilane as the internal standard). Mass spectra were measured on Thermo Scientific ITQ 1100™ GC/MSn. Elemental analyses were carried out with a vario MICRO cube elementar. Ultrasound irradiation was performed on a Kun Shan KQ-3200 B ultrasound cleaner (maximum power, 150 W, 40 kHz). Scanning electron microscope (SEM) images were collected on a JEOL JEM-6700F at 3 KV, with the samples sputtered with a layer of platinum (*ca*. 2 nm thick) prior to imaging to improve conductivity. Powder X-ray diffraction (XRD) patterns were recorded on a Rigaku D/MAX 2500/PC X-ray diffractometer with CuKα radiation (λ = 0.15418 nm). FT-IR spectra and temperature-dependent FT-IR spectra were recorded on a Bruker Optics VERTEX 80v Fourier transform infrared spectrometer, equipped with a DTGS detector in pressed KBr pellets. UV–vis absorption spectra were measured on a Shimadzu 3600 UV–vis–near-IR recording spectrophotometer using 2 nm slit width. The UV–vis diffuse reflectance spectra are taken on a Shimadzu 3600 UV–vis–near-IR recording spectrophotometer using a 20 nm slit width and $BaSO_4$ as the reference. The crystal data collection was performed on a Rigaku RAXIS-RAPID equipped with a narrow-focus, 5.4 KW sealed tube X-ray source (graphite-monochromated Mo Kα radiation, λ = 0.71073 Å). The structure was then refined on F^2 using SHELXL-97.

Synthesis of *N*,*N*′-bis(4-(2-cyano-2-phenylvinyl)phenyl)-5-nitroisophthalamide (BPNIA). 5-Nitro-isophthaloyl dichloride and 2-phenyl-3-(*p*-aminophenyl)acrylonitrile (PAPAN) were synthesized according to the published methods.[23] PAPAN (1.28 g, 5.82 mmol) and triethylamine (0.80 mL, 5.77 mmol) were added to a solution of 5-nitro-isophthaloyl dichloride (0.48 g, 1.94 mmol) in dried dichloromethane (25 mL). The reaction mixture was stirred at room temperature under nitrogen atmosphere for 20 h with plenty of pale yellow precipitate emerging. The precipitate was filtered and washed several times with CH_2Cl_2 and THF, respectively, to obtain a yellow solid as product (1.10 g, yield 92%). UV–vis (DMSO) λ_{max} (nm): 355. ^{1}H NMR (500 MHz, DMSO): δ 11.14 (s, 2H), 9.13 (s, 1H), 8.99 (s, 2H), 8.06–8.01 (m, 10H), 7.78 (d, J = 7.0 Hz, 4H), 7.53 (t, J = 7.5 Hz, 4H), 7.45 (t, J = 7.5 Hz, 2H). FT-IR (KBr) ν_{max}/cm^{-1}: 3342 (NH), 3096, 3084, 3032, 2217(CN), 1683, 1594, 1519, 1449, 1412, 1322, 1250, 1184. Anal. Calcd for $C_{38}H_{25}N_5O_4$: C, 74.14; H, 4.09; N, 11.38. Found: C, 74.27; H, 4.09; N, 11.67. MS: m/z = 615.41.

Experimental details for anion sensing

For the UV–vis experiments, the concentration of BPNIA solution was 10 μM in DMSO. Aliquots of a fresh tetrabutylammonium (TBA) salt standard solution of the envisaged anion (F^-, Cl^-, Br^-, I^-, $H_2PO_4^-$, AcO^-) were added, and the UV–vis absorption spectra of the samples were recorded. ^1H NMR titrations were carried out with the receptor BPNIA (6.5 mM) in DMSO. For the naked-eye sensing test of the DMSO gel of BPNIA, 2 equiv of solid TBAF was dropped on the top of the gel.

Acknowledgements

This work was supported by the National Basic Research Program of China (2012CB933803) and the National Natural Science Foundation of China (20874038).

Notes and references

1 (*a*) M.-O. M. Piepenbrock, G. O. Lloyd, N. Clarke and J. W. Steed, *Chem. Rev.*, 2010, **110**, 1960–2004; (*b*) M. George and R. G. Weiss, *Acc. Chem. Res.*, 2006, **39**, 489–497; (*c*) N. M. Sangeetha and U. Maitra, *Chem. Soc. Rev.*, 2005, **34**, 821–836; (*d*) P. Terech and R. G. Weiss, *Chem. Rev.*, 1997, **97**, 3133–3159.

2 (*a*) A. Ajayaghosh and V. K. Praveen, *Acc. Chem. Res.*, 2007, **40**, 644–656; (*b*) H. Yang, T. Yi, Z. G. Zhou, Y. F. Zhou, J. C. Wu, M. Xu, F. Y. Li and C. H. Huang, *Langmuir*, 2007, **23**, 8224–8230; (*c*) C. Wang, D. Q. Zhang and D. B. Zhu, *J. Am. Chem. Soc.*, 2005, **127**, 16372–16373; (*d*) M. Suzuki, Y. Nakajima, M. Yumoto, M. Kimura, H. Shirai and K. Hanabusa, *Langmuir*, 2003, **19**, 8622–8624.

3 Y. G. Li, K. G. Liu, J. Liu, J. X. Peng, X. L. Feng and Y. Fang, *Langmuir*, 2006, **22**, 7016–7020.

4 (*a*) G. O. Lloyd and J. W. Steed, *Nat. Chem.*, 2009, **1**, 437–442; (*b*) H. Maeda, *Chem.–Eur. J.*, 2008, **14**, 11274–11282; (*c*) J. E. A. Webb, M. J. Crossley, P. Turner and P. Thordarson, *J. Am. Chem. Soc.*, 2007, **129**, 7155–7162.

5 S.-I. Kawano, N. Fujita and S. Shinkai, *J. Am. Chem. Soc.*, 2004, **126**, 8592–8593.

6 (*a*) M. Yoshio, Y. Shoji, Y. Tochigi, Y. Nishikawa and T. Kato, *J. Am. Chem. Soc.*, 2009, **131**, 6763–6767; (*b*) I. O. Shklyarevskiy, P. Jonkheijm, P. C. M. Christianen, A. P. H. J. Schenning, A. D. Guerzo, J.-P. Desvergne, E. W. Meijer and J. C. Maan, *Langmuir*, 2005, **21**, 2108–2112.

7 (*a*) J. H. Kim, M. Seo, Y. J. Kim and S. Y. Kim, *Langmuir*, 2009, **25**, 1761–1766; (*b*) S. Wang, W. Shen, Y. L. Feng and H. Tian, *Chem. Commun.*, 2006, 1497–1499.

8 T. Naota and H. Koori, *J. Am. Chem. Soc.*, 2005, **127**, 9324–9325.

9 (*a*) K. L. Kirk, *Biochemistry of the Halogens and Inorganic Halides*, Plenum Press, New York, 1991, p. 58; (*b*) B. L. Riggs, *Bone and Mineral Research; Annual 2*, Elsevier, Amsterdam, 1984, pp. 366–393.

10 (*a*) S. K. Dey and G. Das, *Chem. Commun.*, 2011, **47**, 4983–4985; (*b*) S. Y. Kim and J.-I. Hong, *Org. Lett.*, 2007, **9**, 3109–3112; (*c*) P. A. Gale, *Acc. Chem. Res.*, 2006, **39**, 465–475; (*d*) T. Gunnlaugsson, M. Glynn, G. M. Tocci, P. E. Kruger and F. M. Pfeffer, *Coord. Chem. Rev.*, 2006, **250**, 3094–3117; (*e*) E. J. Cho, J. W. Moon, S. W. Ko, J. Y. Lee, S. K. Kim, J. Yoon and K. C. Nam, *J. Am. Chem. Soc.*, 2003, **125**, 12376–12377; (*f*) T. Gunnlaugsson, A. P. Davis, G. M. Hussey, J. Tierney and M. Glynn, *Org. Biomol. Chem.*, 2004, **2**, 1856–1863.

11 (*a*) J. J. Park, Y.-H. Kim, C. Kim and J. Kang, *Tetrahedron Lett.*, 2011, **52**, 3361–3366; (*b*) X. P. Bao, J. H. Yu and Y. H. Zhou, *Sens. Actuators, B*, 2009, **140**, 467–472; (*c*) J. Yoo, M.-S. Kim, S.-J. Hong, J. L. Sessler and C.-H. Lee, *J. Org. Chem.*, 2009, **74**, 1065–1069; (*d*) K. S. Moon, N. Singh, G. W. Lee and D. O. Jang, *Tetrahedron*, 2007, **63**, 9106–9111; (*e*) E. Quinlan, S. E. Matthews and T. Gunnlaugsson, *J. Org. Chem.*, 2007, **72**, 7497–7503; (*f*) H. J. Kim, S. K. Kim, J. Y. Lee and J. S. Kim, *J. Org. Chem.*, 2006, **71**, 6611–6614; (*g*) B. Liu and H. Tian, *J. Mater. Chem.*, 2005, **15**, 2681–2686.

12 (*a*) P. Rajamalli and E. Prasad, *Org. Lett.*, 2011, **13**, 3714–3717; (*b*) D. F. Xu, X. L. Liu, R. Lu, P. C. Xue, X. F. Zhang, H. P. Zhou and J. H. Jia, *Org. Biomol. Chem.*, 2011, **9**, 1523–1528; (*c*) J.-W. Liu, Y. Yang, C.-F. Chen and J.-T. Ma, *Langmuir*, 2010, **26**, 9040–9044; (*d*) Y.-M. Zhang, Q. Lin, T.-B. Wei, X.-P. Qin and Y. Li, *Chem. Commun.*, 2009, 6074–6076; (*e*) M. J. Teng, G. C. Kuang, X. R. Jia, M. Gao, Y. Li and Y. Wei, *J. Mater. Chem.*, 2009, **19**, 5648–5654; (*f*) Z. Džolić, M. Cametti, A. D. Cort, L. Mandolini and M. Žinić, *Chem. Commun.*, 2007, 3535–3537; (*g*) C. Wang, D. Q. Zhang and D. B. Zhu, *Langmuir*, 2007, **23**, 1478–1482; (*h*) M. Yamanaka, T. Nakamura, T. Nakagawa and H. Itagaki, *Tetrahedron Lett.*, 2007, **48**, 8990–8993.

13 B.-K. An, D.-S. Lee, J.-S. Lee, Y.-S. Park, H.-S. Song and S. Y. Park, *J. Am. Chem. Soc.*, 2004, **126**, 10232–10233.

14 C. Suksai and T. Tuntulani, *Chem. Soc. Rev.*, 2003, **32**, 192–202.

15 (*a*) Y. G. Li, T. Y. Wang and M. H. Liu, *Tetrahedron*, 2007, **63**, 7468–7473; (*b*) T. Naota and H. Koori, *J. Am. Chem. Soc.*, 2005, **127**, 9324–9325; (*c*) G. Cravotto and P. Cintas, *Chem. Soc. Rev.*, 2009, **38**, 2684–2697.

16 J. E. Eldridge and J. D. Ferry, *J. Phys. Chem.*, 1954, **58**, 992–995.

17 D. Oelkrug, A. Tompert, J. Gierschner, H.-J. Egelhaaf, M. Hanack, M. Hohloch and E. Steinhuber, *J. Phys. Chem. B*, 1998, **102**, 1902–1907.

18 S.-J. Yoon, J. H. Kim, J. W. Chung and S. Y. Park, *J. Mater. Chem.*, 2011, **21**, 18971–18973.

19 (*a*) P. A. Gale, S. E. García-Garrido and J. Garric, *Chem. Soc. Rev.*, 2008, **37**, 151–190; (*b*) C. R. Bondy and S. J. Loeb, *Coord. Chem. Rev.*, 2003, **240**, 77–99.

20 S. Gronert, *J. Am. Chem. Soc.*, 1993, **115**, 10258–10266.

21 I. G. Shenderovich, H.-H. Limbach, S. N. Smirnov, P. M. Tolstoy, G. S. Denisov and N. S. Golubev, *Phys. Chem. Chem. Phys.*, 2002, **4**, 5488–5497.

22 (*a*) X. M. He, S. Z. Hu, K. Liu, Y. Guo, J. Xu and S. J. Shao, *Org. Lett.*, 2006, **8**, 333–336; (*b*) M. Boiocchi, L. Del Boca, D. E. Gomez, L. Fabbrizzi, M. Licchelli and E. Monzani, *J. Am. Chem. Soc.*, 2004, **126**, 16507–16514.

23 (*a*) Y.-S. Zheng and Y.-J. Hu, *J. Org. Chem.*, 2009, **74**, 5660–5663; (*b*) S. Coco, C. Cordovilla, B. Donnio, P. Espinet, M. J. García-Casas and D. Guillon, *Chem.–Eur. J.*, 2008, **14**, 3544–3552.